

# Thermal neutron capture cross sections for $^{16,17,18}\text{O}$ and $^2\text{H}$

R. B. Firestone<sup>1,\*</sup> and Zs. Revay<sup>2,3</sup>

<sup>1</sup>*University of California, Department of Nuclear Engineering, Berkeley, California 94720, USA*

<sup>2</sup>*Nuclear Analysis and Radiography Department, Center for Energy Research, Hungarian Academy of Sciences, P.O. Box 49, H-Budapest 1525, Hungary*

<sup>3</sup>*Heinz Maier-Leibnitz Zentrum (MLZ), Technische Universität München, D-85747 Garching, Germany*

(Received 8 October 2015; revised manuscript received 18 February 2016; published 12 April 2016)

Thermal neutron capture  $\gamma$ -ray spectra for  $^{16,17,18}\text{O}$  and  $^2\text{H}$  have been measured with guided cold neutron beams from the Forschungs-Neutronenquelle Heinz Maier-Leibnitz (FRM II) reactor and the Budapest Research Reactor (BRR) on natural and  $^{17,18}\text{O}$  enriched  $\text{D}_2\text{O}$  targets. Complete neutron capture  $\gamma$ -ray decay schemes for the  $^{16,17,18}\text{O}(n,\gamma)$  reactions were measured. Absolute transition probabilities were determined for each reaction by a least-squares fit of the  $\gamma$ -ray intensities to the decay schemes after accounting for the contribution from internal conversion. The transition probability for the 870.76-keV  $\gamma$  ray from  $^{16}\text{O}(n,\gamma)$  was measured as  $P_\gamma(871) = 96.6 \pm 0.5\%$  and the thermal neutron cross section for this  $\gamma$  ray was determined as  $0.164 \pm 0.003$  mb by internal standardization with multiple targets containing oxygen and stoichiometric quantities of hydrogen, nitrogen, and carbon whose  $\gamma$ -ray cross sections were previously standardized. The  $\gamma$ -ray cross sections for the  $^{17,18}\text{O}(n,\gamma)$  and  $^2\text{H}(n,\gamma)$  reactions were then determined relative to the 870.76-keV  $\gamma$ -ray cross section after accounting for the isotopic abundances in the targets. We determined the following total radiative thermal neutron cross sections for each isotope from the  $\gamma$ -ray cross sections and transition probabilities;  $\sigma_0(^{16}\text{O}) = 0.170 \pm 0.003$  mb;  $\sigma_0(^{17}\text{O}) = 0.67 \pm 0.07$  mb;  $\sigma_0(^{18}\text{O}) = 0.141 \pm 0.006$  mb; and  $\sigma_0(^2\text{H}) = 0.489 \pm 0.006$  mb.

DOI: [10.1103/PhysRevC.93.044311](https://doi.org/10.1103/PhysRevC.93.044311)

## I. INTRODUCTION

The hydrogen and deuterium thermal neutron cross sections are very important for many nuclear applications including neutron moderation and the design of heavy water reactors. Oxygen is the most abundant element in Earth's crust and, despite its low thermal neutron cross section, it remains an important component of many neutron transport calculations. The deuterium and oxygen thermal neutron cross sections are among the smallest of all isotopes and they are difficult to measure because of interference from other, higher cross-section materials. Measurement of the thermal neutron cross sections for the lower abundance  $^2\text{H}$  and  $^{17,18}\text{O}$  isotopes requires the use of isotopically enriched targets.

In this work we have employed the prompt gamma-ray activation analysis (PGAA) method [1] using guided neutron beams from the 20 MW FRM II [2,3] and 10 MW BRR [4] reactors to measure the total radiative thermal neutron cross sections for  $^{16,17,18}\text{O}$  and  $^2\text{H}$ . The PGAA method is advantageous over other techniques because the prompt  $\gamma$ -ray cross sections can be internally calibrated using compounds of well-known stoichiometry containing isotopes with standardized  $\gamma$ -ray cross sections. For the lightest elements PGAA can measure complete neutron capture  $\gamma$ -ray decay schemes from which the absolute transition probabilities can be determined. The total thermal radiative neutron capture cross sections can then be determined from the  $\gamma$ -ray cross sections and the absolute transition probabilities. The  $^{18}\text{O}(n,\gamma)$  cross section can also be determined from the short-lived  $^{19}\text{O}$  ( $t_{1/2} = 28.66$  s)  $\gamma$ -ray decay cross sections and transition probabilities observed in the prompt spectrum.

## II. EXPERIMENT

Neutron capture  $\gamma$ -ray energies, intensities, and cross sections were measured with the guided neutron beams at the PGAA facilities of the FRM II and BRR reactors. The target stations were 51 m and 30 m from the reactor core and the neutron flux was  $3 \times 10^{10} \text{ cm}^{-2}\text{s}^{-1}$  and  $5 \times 10^7 \text{ cm}^{-2}\text{s}^{-1}$  at the FRM II and BRR reactors, respectively. Prompt gamma rays from the target were measured at both facilities with n-type high-purity, 60% efficient, germanium (HPGe) detectors surrounded by an annulus of eight BGO scintillators connected in anticoincidence mode for Compton suppression. A lead collimator was placed in front of the detector to focus  $\gamma$  rays, irradiated by the neutron beam, on to the detector. Counting efficiency was calibrated from 50 keV to 10 MeV with radioactive sources and  $(n,\gamma)$  reaction  $\gamma$  rays to a precision of better than 1% from 500 keV to 6 MeV and better than 3% at all other energies [5]. The  $\gamma$ -ray spectra were analyzed with the Hypermet PC [5,6] peak analysis code.

### A. Standardization

Standardization of the 870.76-keV  $\gamma$  ray from  $^{16}\text{O}(n,\gamma)$  was performed by measuring the prompt  $\gamma$ -ray spectra from  $\text{H}_2\text{O}$ , urea  $\text{CH}_4\text{N}_2\text{O}$ , and  $\text{Pb}(\text{NO}_3)_2$  targets. The data were standardized with respect to the 2223.2487-keV  $\gamma$  ray from  $^1\text{H}(n,\gamma)$ , the 4945.30 keV  $\gamma$  ray from  $^{12}\text{C}(n,\gamma)$ , and the 1884.85 keV  $\gamma$  ray from  $^{14}\text{N}(n,\gamma)$ . These  $\gamma$ -ray cross sections are shown in Table I. The hydrogen  $\gamma$ -ray cross section is derived from the recommended [7] total radiative thermal neutron cross section,  $\sigma_0(^1\text{H}) = 332.6 \pm 0.7$  mb [7], corrected for internal pair formation (IPF), where  $\alpha_{\text{IPF}} = 3.32(5) \times 10^{-4}$  [8]. The 870.76-keV  $\gamma$ -ray cross sections derived from these standardizations are shown in Table I. The weighted average

\*rbfirestone@lbl.gov

TABLE I. Standardization of the 870.76-keV  $\gamma$  ray from  $^{16}\text{O}(n,\gamma)$ . Measurements were performed on multiple samples of the urea and  $\text{Pb}(\text{NO}_3)_2$  targets.

Standard	$E_\gamma$ (keV)	$\sigma_\gamma$ (std)	$\sigma_\gamma$ (871) (mb)
$\text{H}_2\text{O}$	2223(H)	$332.5 \pm 0.7$	$0.161 \pm 0.003$
Urea-1	1885(N)	$14.57 \pm 0.04$	$0.168 \pm 0.006$
Urea-2	1885(N)	$14.57 \pm 0.04$	$0.170 \pm 0.008$
Urea-2	2223(H)	$332.5 \pm 0.7$	$0.168 \pm 0.007$
Urea-2	4945(C)	$2.62 \pm 0.03$	$0.163 \pm 0.008$
$\text{Pb}(\text{NO}_3)_2$ -1	1885(N)	$14.57 \pm 0.04$	$0.155 \pm 0.006$
$\text{Pb}(\text{NO}_3)_2$ -2	1885(N)	$14.57 \pm 0.04$	$0.162 \pm 0.007$
	Weighted average		$0.164 \pm 0.003$

of seven measurements is  $\sigma_0(871) = 0.164 \pm 0.003$  mb with a  $\chi^2/f=0.54$ . A high level of confidence can be accorded to this result because of the number of self-consistent values obtained through multiple independent calibrations. This  $\gamma$  ray was used to standardize the cross sections from the  $^{17,18}\text{O}(n,\gamma)$  and  $^2\text{H}(n,\gamma)$  reactions.

### B. Cross-section measurements

The  $^2\text{H}$  and  $^{16,17,18}\text{O}$  thermal neutron capture  $\gamma$ -ray intensities were measured using a natural and two  $^{17,18}\text{O}$  enriched  $\text{D}_2\text{O}$  targets whose compositions are described in Table II. The  $^{17,18}\text{O}$  enriched targets were provided by the Paul Scherrer Institut and were calibrated using a sector field mass spectrometer. The targets were  $\approx 3$ -mm thick and corrections for  $\gamma$ -ray attenuation were only necessary for  $E_\gamma < 100$  keV. As discussed later in this paper all  $\gamma$  rays observed were  $> 500$  keV, requiring no correction, except for two low energy transitions in  $^{19}\text{O}$  whose intensities could be confirmed by intensity balances. Both targets were irradiated for 118 801 s. The deuterated targets were enriched to  $> 99.9\%$  in deuterium. The  $\gamma$ -ray cross sections  $\sigma_\gamma$  for  $^{17,18}\text{O}(n,\gamma)$  and  $^2\text{H}(n,\gamma)$  reactions were then determined from their intensity ratio to the 870.76-keV  $\gamma$  ray from  $^{16}\text{O}(n,\gamma)$  after accounting for the target isotopic abundances.

Each of the  $(n,\gamma)$  decay schemes discussed here is complete, as indicated by the intensity balance through the level scheme. The absolute transition probabilities,  $P_\gamma(\%)$ , were determined by a least-squares fit of  $\gamma$ -ray intensities to the level scheme, constrained so that for the capture state (CS) de-exciting and ground-state (GS) feeding transitions  $\Sigma_\gamma(\text{CS}) = \Sigma_\gamma(\text{GS}) = 100.0$  and  $\Sigma_\gamma(\text{populating}) - \Sigma_\gamma(\text{depopulating}) = 0$  for the intermediate levels. The transition intensities were

TABLE II.  $\text{D}_2\text{O}$  target compositions used in these experiments. All targets were  $> 99.9\%$  enriched in  $^2\text{H}$ .

Target	$\%^{16}\text{O}$	$\%^{17}\text{O}$	$\%^{18}\text{O}$
Natural target	$99.757 \pm 0.016$	$0.038 \pm 0.001$	$0.205 \pm 0.014$
Enriched target-1	$50.1 \pm 1.6$	$15.4 \pm 1.7$	$34.6 \pm 1.8$
Enriched target-2	$58.5 \pm 1.6$	$10.2 \pm 1.7$	$31.2 \pm 1.8$

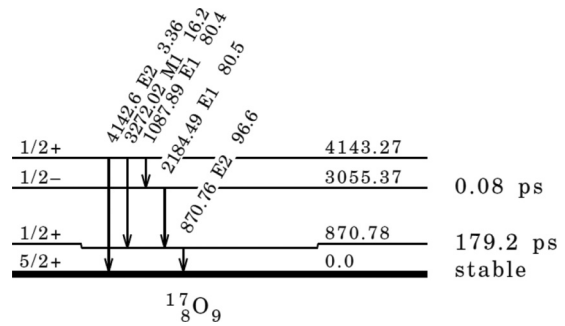


FIG. 1. The  $^{17}\text{O}$  level scheme produced by the  $^{16}\text{O}(n,\gamma)$  reaction. Total transition probabilities  $I_{\gamma+e}$  are shown.

corrected for internal conversion, which is dominated by internal pair formation (IPF) at high energies, calculated with the computer code BRICC [8].

The total radiative thermal neutron capture cross sections could then be calculated from the  $\gamma$ -ray cross sections  $\sigma_\gamma$ , and the transition probabilities  $P_\gamma$ , by Eq. (1):

$$\sigma_0 = 100 \times \frac{\sigma_\gamma}{P_\gamma(\%)}. \quad (1)$$

The uncertainties in the total radiative thermal neutron cross sections arise from the uncertainty in the standardization  $\gamma$ -ray cross section, shown in Table I, statistical uncertainty in the  $\gamma$ -ray peak analysis, and uncertainty in the isotopic branching ratios of the target.

### I. $^{16}\text{O}(n,\gamma)$ cross section

A  $\text{D}_2\text{O}^{\text{nat}}$  target was irradiated for 83 060 s in the cold neutron beam at the FRM-II reactor. Five  $\gamma$  rays were placed in the  $^{16}\text{O}(n,\gamma)$  level scheme and are shown in Fig. 1. The  $\gamma$ -ray intensities were fitted to the level scheme determining the transition probabilities with a  $\chi^2/f=0.74$  which are summarized in Table III. The  $^{16}\text{O}$  total radiative neutron capture cross section was determined from Eq. (1) as  $\sigma_0(^{16}\text{O}) = 0.170 \pm 0.003$  mb based upon  $\sigma_\gamma(872) = 0.164 \pm 0.03$  mb and  $P_\gamma(872) = 96.6 \pm 0.5\%$ . This value is consistent with  $0.178 \pm 0.025$  mb, measured by Journey [10], but it is lower than  $0.202 \pm 0.028$  mb, from McDonald *et al.* [11], and  $0.187 \pm 0.010$  mb, from Wüst *et al.* [12]. The McDonald *et al.* measurement was standardized assuming  $\sigma_0(^2\text{H}) = 0.521 \pm 0.009$  mb, however, using our new value  $0.489 \pm 0.006$  mb, discussed below, their value becomes  $0.190 \pm 0.026$  mb which is consistent with our measurement. The Wüst *et al.* value assumes  $P_\gamma$

TABLE III.  $\gamma$ -ray energies, intensities, and transition probabilities for the  $^{16}\text{O}(n,\gamma)$  reaction.

$E_\gamma$ (keV)	Mult	ICC	$I_\gamma$	$P_\gamma(\%)^a$
$870.76 \pm 0.08$	E2	$8.85 \times 10^{-6}$	$100.0 \pm 0.8$	$96.6 \pm 0.5$
$1087.86 \pm 0.08$	E1	$2.31 \times 10^{-6}$	$83.8 \pm 0.6$	$80.4 \pm 0.5$
$2184.44 \pm 0.09$	E1	$7.7 \times 10^{-4}$	$84.8 \pm 1.2$	$80.4 \pm 0.5$
$3272.15 \pm 0.10$	M1	$7.6 \times 10^{-4}$	$16.9 \pm 0.5$	$16.2 \pm 0.4$
$4142.73 \pm 0.13$	E2	0.00122	$3.5 \pm 0.3$	$3.36 \pm 0.24$

<sup>a</sup>Constrained least-squares fit to the level scheme with a  $\chi^2/f=0.74$ .

TABLE IV.  $\gamma$ -ray intensities and transition probabilities for the  $^{17}\text{O}(n,\gamma)$  reaction.

$E_\gamma$ (keV)	Mult	ICC	$I_\gamma$			$P_\gamma(\%)$	Comment
			Target-1	Target-2	Average	Fit <sup>a</sup>	
536.24 ± 0.22	E1	1.10 × 10 <sup>-5</sup>	1.5 ± 0.6		1.5 ± 0.4	1.5 ± 0.3	
797.9 ± 0.4	E1	4.31 × 10 <sup>-6</sup>	0.46 ± 0.23		0.46 ± 0.23	0.26 ± 0.19	b
822.25 ± 0.06	E1	4.04 × 10 <sup>-6</sup>	31.2 ± 2.4	25 ± 3	28.5 ± 1.8	24.9 ± 0.5	c
861.7 ± 0.4	E1	3.66 × 10 <sup>-6</sup>	0.16 ± 0.04		0.16 ± 0.04	0.14 ± 0.03	b
880.4 ± 0.4	E1	3.50 × 10 <sup>-6</sup>	0.41 ± 0.06		0.41 ± 0.06	0.35 ± 0.05	b
944.2 ± 0.4	E1	3.04 × 10 <sup>-6</sup>	0.53 ± 0.07		0.53 ± 0.07	0.47 ± 0.06	b
1074.27 ± 0.16	M1	3.46 × 10 <sup>-6</sup>	1.9 ± 0.5		1.9 ± 0.5	1.7 ± 0.4	
1177.8 ± 0.4	E1	4.76 × 10 <sup>-5</sup>	2.4 ± 0.6	1.6 ± 0.8	2.1 ± 0.5	2.3 ± 0.4	
1334.1 ± 0.4	M1	2.78 × 10 <sup>-5</sup>	1.5 ± 0.4	2.3 ± 0.8	1.7 ± 0.4	1.2 ± 0.3	
1457.69 ± 0.22	M1	5.34 × 10 <sup>-5</sup>	2.6 ± 0.6		2.6 ± 0.6	2.1 ± 0.4	
1542.6 ± 0.3	E1	3.03 × 10 <sup>-4</sup>	0.6 ± 0.2		0.6 ± 0.2	0.7 ± 0.2	b,c
1572.98 ± 0.16	E2	1.20 × 10 <sup>-4</sup>	8.9 ± 0.6	8.3 ± 0.8	8.7 ± 0.5	6.3 ± 0.3	
1610.5 ± 0.3	E1	3.57 × 10 <sup>-4</sup>	1.5 ± 0.5		1.5 ± 0.5	1.5 ± 0.4	b
1620.1 ± 0.4	E2	1.40 × 10 <sup>-4</sup>	0.18 ± 0.10		0.18 ± 0.10	0.14 ± 0.09	b
1651.77 ± 0.05	E2	1.53 × 10 <sup>-4</sup>	29.0 ± 0.6	26 ± 3	28.9 ± 0.6	25.3 ± 0.5	
1695.85 ± 0.08	E1	4.23 × 10 <sup>-4</sup>	14.2 ± 0.8	22 ± 3	14.8 ± 0.8	12.5 ± 0.6	
1698.9 ± 0.4	E2	1.74 × 10 <sup>-4</sup>	0.18 ± 0.10		0.18 ± 0.10	0.17 ± 0.09	b
1742.03 ± 0.13	M1	1.44 × 10 <sup>-4</sup>	0.60 ± 0.07		0.60 ± 0.07	0.52 ± 0.06	
1847.53 ± 0.1	E1	5.35 × 10 <sup>-4</sup>	13.4 ± 0.8	18.1 ± 1.3	14.7 ± 0.7	12.8 ± 0.4	
1893.71 ± 0.11	M1	2.01 × 10 <sup>-4</sup>	1.4 ± 0.5		1.4 ± 0.5	1.7 ± 0.4	b
1937.77 ± 0.22	M1	2.18 × 10 <sup>-4</sup>	20.9 ± 1.8	20.2 ± 2.3	20.1 ± 1.4	16.3 ± 0.9	
1982.06 ± 0.05	E2	3.06 × 10 <sup>-4</sup>	100.0 ± 2.0	100 ± 4	100.0 ± 1.8	85.8 ± 1.1	
2429.89 ± 0.23	E1	9.28 × 10 <sup>-4</sup>	10.5 ± 1.6	11 ± 3	10.8 ± 1.4	7.2 ± 0.7	c
2473.94 ± 0.06	E1	9.56 × 10 <sup>-4</sup>	14.6 ± 0.6	23.0 ± 1.0	16.8 ± 0.5	14.8 ± 0.4	c
2515.25 ± 0.15	E1	9.82 × 10 <sup>-4</sup>	6.7 ± 0.5		6.7 ± 0.5	5.9 ± 0.4	b
2564.2 ± 0.14	E1	0.00101	0.37 ± 0.05		0.37 ± 0.05	0.32 ± 0.04	
2668.03 ± 0.08	M1	5.20 × 10 <sup>-4</sup>	13.4 ± 0.6	8 ± 4	13.2 ± 0.6	11.7 ± 0.4	
2709.1 ± 0.4	E2	6.55 × 10 <sup>-4</sup>	0.81 ± 0.20	1.0 ± 0.3	0.81 ± 0.20	0.73 ± 0.09	
2791.6 ± 0.4	M1	5.71 × 10 <sup>-4</sup>	2.2 ± 0.4	1.8 ± 0.5	2.1 ± 0.3	1.94 ± 0.23	
2947.9 ± 0.3	E1	0.00121	10.3 ± 1.2	10.6 ± 0.8	10.5 ± 0.7	9.0 ± 0.5	
3115.5 ± 0.3	E1	0.00199	6.3 ± 0.8		6.3 ± 0.8	6.1 ± 0.5	
3271.7 ± 0.4	M1+E2	7.62 × 10 <sup>-4</sup>	0.8 ± 0.4	0.8 ± 0.5	0.8 ± 0.3	0.60 ± 0.23	c
3354.2 ± 0.4	E2	9.33 × 10 <sup>-4</sup>	0.59 ± 0.10		0.59 ± 0.10	0.51 ± 0.08	b
3395.29 ± 0.11	M1	8.06 × 10 <sup>-4</sup>	11.6 ± 0.5	9.8 ± 0.8	11.1 ± 0.4	9.6 ± 0.3	
3548.06 ± 0.16	E1	0.0015	2.9 ± 0.5		2.9 ± 0.5	2.6 ± 0.4	
3589.37 ± 0.08	E1	0.00152	44 ± 4	44 ± 5	44 ± 3	36.7 ± 1.2	c
3633.64 ± 0.07	E0		0.087 ± 0.018		0.087 ± 0.018	0.076 ± 0.015	b
3919.6 ± 0.22	E2	0.00114	3.3 ± 0.4		3.3 ± 0.4	2.7 ± 0.3	
4125.49 ± 0.22	M1	0.00106	3.4 ± 0.5	4.7 ± 1.0	3.6 ± 0.5	3.2 ± 0.4	
4367.38 ± 0.12	E1	0.00182	3.8 ± 0.5		3.8 ± 0.5	3.6 ± 0.4	
4490.22 ± 0.17	M1	0.00118	4.9 ± 0.6		4.9 ± 0.6	5.4 ± 0.4	
6197.28 ± 0.14	E1	0.00234	12.0 ± 0.8	16.0 ± 1.3	13.1 ± 0.7	11.4 ± 0.4	c

<sup>a</sup>Constrained least-squares fit to the level scheme with a  $\chi^2/\text{f} = 1.22$ .<sup>b</sup>From ENSDF adopted levels, gammas [9].<sup>c</sup>Cross section corrected for contaminant contribution.

(872) =  $82 \pm 3\%$  and correcting this for our newer value gives  $0.159 \pm 0.006$  mb, slightly lower than our value.

The neutron separation energy determined in this experiment,  $S_n = 4143.27 \pm 0.13$  keV, is slightly higher than

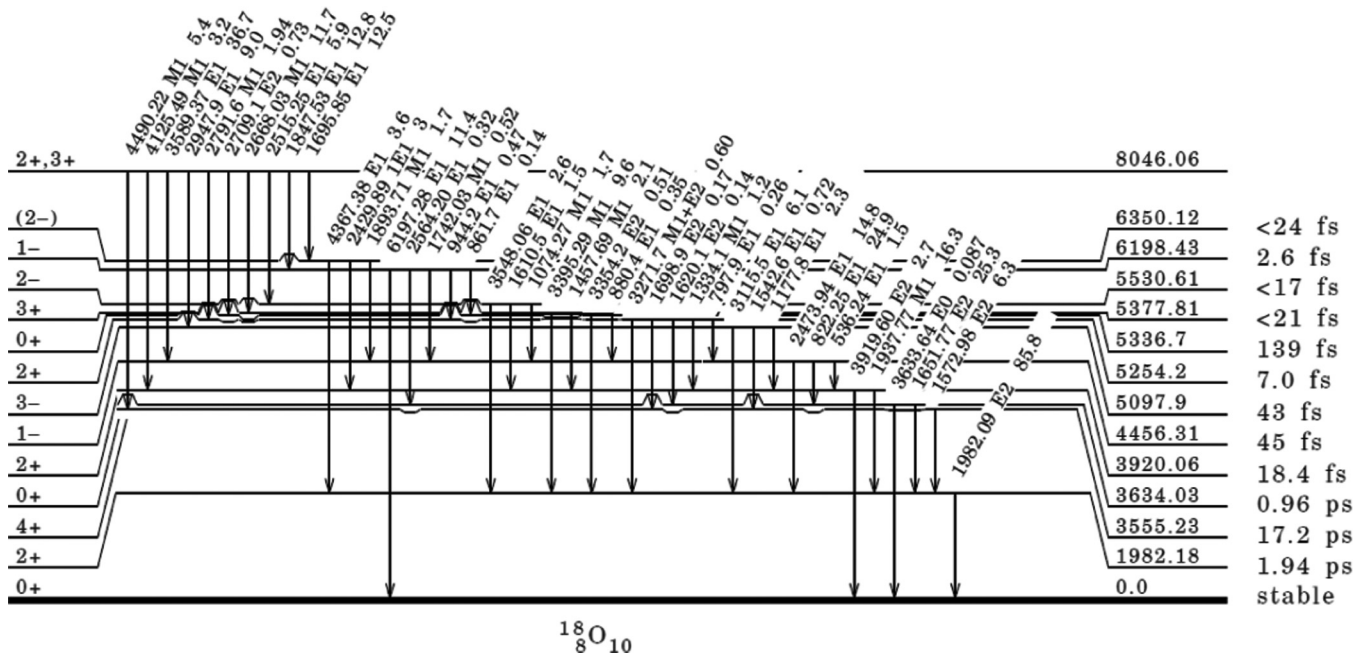


FIG. 2. The  $^{18}\text{O}$  level scheme produced by the  $^{17}\text{O}(n,\gamma)$  reaction. Total transition probabilities  $I_{\gamma+e}$  are shown.

the  $4143.079 \pm 0.001$  keV value recommended by the atomic mass evaluation [13].

2.  $^{17}\text{O}(n,\gamma)$  cross section

The neutron capture decay scheme for the  $^{17}\text{O}(n,\gamma)$  reaction is shown in Fig. 2. It consists of 42  $\gamma$  rays including 12 weak transitions, not observed here, that were adopted from the ENSDF adopted levels, gammas [9]. The  $\gamma$ -ray intensities measured on the two targets and the transition probabilities, fitted with a  $\chi^2/f=1.22$ , are summarized in Table IV. The

$\gamma$ -ray cross sections measured for the more intense transitions on each target are shown in Table V. The total radiative thermal neutron cross sections,  $\sigma_0(^{17}\text{O})$ , calculated for each  $\gamma$  ray, are consistent for each target giving a weighted average value of  $\sigma_0(^{17}\text{O}) = 0.64 \pm 0.08$  mb for Target-1 and  $\sigma_0(^{17}\text{O}) = 0.76 \pm 0.13$  mb for Target-2. Both targets have a statistical uncertainty of 1.4% and a standardization uncertainty of 4%, but the main source of uncertainty is from the  $^{17}\text{O}$  abundance in each target, 12% for Target-1 and 17% for Target-2. The weighted average total radiative neutron cross section from both measurements is  $\sigma_0(^{17}\text{O}) = 0.67 \pm 0.07$  mb. This value is consistent with the

TABLE V.  $^{17}\text{O}(n,\gamma)$   $\gamma$ -ray cross sections measurements and the  $^{17}\text{O}$  total radiative neutron cross section.

$E_\gamma$ (keV)	Target-1 (mb)		Target-2 (mb)	
	$\sigma_\gamma$	$\sigma_0$	$\sigma_\gamma$	$\sigma_0$
$822.25 \pm 0.06$	$0.176 \pm 0.014$	$0.71 \pm 0.07$	$0.242 \pm 0.019$	$0.85 \pm 0.07$
$1651.77 \pm 0.05$	$0.163 \pm 0.003$	$0.65 \pm 0.02$	$0.225 \pm 0.005$	$0.78 \pm 0.02$
$1695.85 \pm 0.08$	$0.080 \pm 0.005$	$0.64 \pm 0.05$	$0.110 \pm 0.006$	$0.74 \pm 0.06$
$1847.53 \pm 0.1$	$0.075 \pm 0.005$	$0.59 \pm 0.05$	$0.104 \pm 0.006$	$0.71 \pm 0.05$
$1937.77 \pm 0.22$	$0.118 \pm 0.010$	$0.72 \pm 0.08$	$0.162 \pm 0.014$	$0.79 \pm 0.08$
$1982.06 \pm 0.05$	$0.563 \pm 0.011$	$0.66 \pm 0.02$	$0.775 \pm 0.016$	$0.78 \pm 0.02$
$2473.94 \pm 0.06$	$0.082 \pm 0.003$	$0.56 \pm 0.03$	$0.113 \pm 0.005$	$0.68 \pm 0.03$
$2515.25 \pm 0.15$	$0.037 \pm 0.003$	$0.64 \pm 0.07$	$0.052 \pm 0.004$	$0.78 \pm 0.08$
$2668.03 \pm 0.08$	$0.075 \pm 0.003$	$0.64 \pm 0.04$	$0.104 \pm 0.005$	$0.78 \pm 0.04$
$2947.9 \pm 0.3$	$0.058 \pm 0.007$	$0.65 \pm 0.09$	$0.080 \pm 0.009$	$0.76 \pm 0.10$
$3115.5 \pm 0.3$	$0.035 \pm 0.005$	$0.58 \pm 0.11$	$0.049 \pm 0.006$	$0.78 \pm 0.12$
$3395.29 \pm 0.11$	$0.065 \pm 0.003$	$0.68 \pm 0.04$	$0.090 \pm 0.004$	$0.81 \pm 0.04$
$3589.37 \pm 0.08$	$0.248 \pm 0.022$	$0.68 \pm 0.08$	$0.341 \pm 0.030$	$0.78 \pm 0.07$
$6197.28 \pm 0.14$	$0.067 \pm 0.005$	$0.59 \pm 0.05$	$0.093 \pm 0.006$	$0.71 \pm 0.05$
	Weighted average	$0.67 \pm 0.07$		$0.76 \pm 0.13$

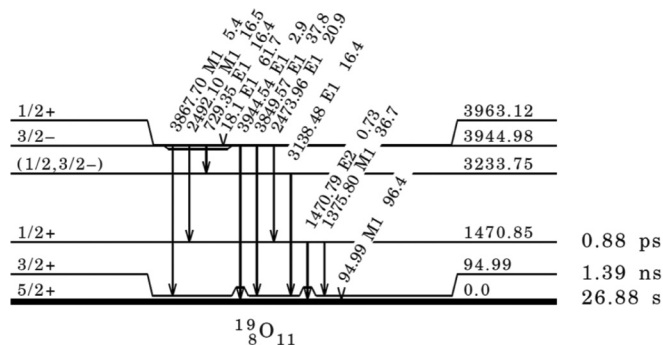


FIG. 3. The  $^{19}\text{O}$  level scheme produced by the  $^{18}\text{O}(n,\gamma)$  reaction. Total transition probabilities  $I_{\gamma+e}$  are shown.

only literature value by Lone and Inglis [14] of  $\sigma_0(^{16}\text{O}) = 0.54 \pm 0.06$  mb.

The neutron separation energy,  $S_n = 8046.06 \pm 0.10$  keV, determined in this experiment is significantly larger than the  $8045.369 \pm 0.001$  keV value reported in the most recent atomic mass evaluation [13].

### 3. $^{18}\text{O}(n,\gamma)$ cross section

The neutron capture decay scheme for the  $^{18}\text{O}(n,\gamma)$  reaction consists of 11  $\gamma$  rays, shown on the level scheme drawing in Fig. 3. The  $\gamma$ -ray intensities, and transition probabilities, fitted with a  $\chi^2/f=1.25$ , are summarized in Table VI. The 18.1-keV transition was not observed in these experiments and its transition probability is calculated from the decay scheme intensity balance as described above. Transition intensity for the 94.94-keV  $\gamma$  ray,  $96.3 \pm 1.2\%$ , was increased by  $2 \pm 1\%$  [1] to account for self-absorption in the target. This transition probability can also be calculated from the intensity balance yielding the remarkably similar value of  $96.3 \pm 1.4\%$ . The  $\gamma$ -ray cross sections for the stronger transitions are summarized in Table VII. The total radiative thermal neutron

TABLE VII.  $^{18}\text{O}(n,\gamma)$   $\gamma$ -ray cross sections measurements and the  $^{18}\text{O}$  total radiative neutron cross section.

$E_\gamma$ (keV)	Target-1	
	$\sigma_\gamma$ (mb)	$\sigma_0$ (mb)
$94.94 \pm 0.09$	$0.138 \pm 0.006$	$0.143 \pm 0.007$
$1375.8 \pm 0.06$	$0.051 \pm 0.003$	$0.140 \pm 0.008$
$2473.96 \pm 0.03$	$0.027 \pm 0.002$	$0.133 \pm 0.012$
$3849.49 \pm 0.15$	$0.052 \pm 0.002$	$0.138 \pm 0.007$
	Target-2	
$1375.8 \pm 0.06$	$0.051 \pm 0.002$	$0.141 \pm 0.011$
$2473.96 \pm 0.03$	$0.029 \pm 0.002$	$0.152 \pm 0.014$
$3849.49 \pm 0.15$	$0.053 \pm 0.002$	$0.142 \pm 0.011$
	Weighted average <sup>a</sup>	$0.142 \pm 0.007$

<sup>a</sup>An additional 6% is added for the uncertainty in the abundance.

cross sections are internally consistent for each target giving a weighted average value of  $\sigma_0(^{18}\text{O}) = 0.140 \pm 0.004$  mb for Target-1 and  $\sigma_0(^{18}\text{O}) = 0.144 \pm 0.007$  mb for Target-2 including 2% and 6% statistical uncertainties for Target-1 and Target-2, respectively, and a 3% standardization uncertainty. The weighted average cross section, adding a 6% uncertainty in the isotopic abundance, is  $0.142 \pm 0.07$  mb.

The  $^{18}\text{O}(n,\gamma)$  cross section can also be determined by activation analysis from  $^{19}\text{O}$   $\beta^-$  decay ( $t_{1/2} = 28.66$  s). We observe the 1357.32-keV  $\gamma$  ray from this decay in the same spectrum as the prompt  $\gamma$  rays. Target-1 gave  $\sigma_\gamma = 0.071 \pm 0.003$  mb and target-2 gave  $\sigma_\gamma = 0.071 \pm 0.005$  mb. From ENSDF we get  $P_\gamma(1357) = 50.4 \pm 1.1\%$  [15]. Target-1 gives  $\sigma_0(^{18}\text{O}) = 0.141 \pm 0.011$  mb and Target-2 gives  $\sigma_0(^{18}\text{O}) = 0.141 \pm 0.014$  mb. The statistical, systematic, and standardization uncertainties for these values are the same as for the prompt  $\gamma$ -ray measurements. The weighted average of

TABLE VI. Transition probabilities for the  $^{18}\text{O}(n,\gamma)$  reaction.

$E_\gamma$ (keV)	Mult	ICC	$I_\gamma$			$P_\gamma(\%)^a$
			Target-1	Target-2	Average	
$18.1 \pm 0.1^b$	E1	0.512				$40.8 \pm 1.2$
$94.94 \pm 0.09$	M1	0.00067	$100.0 \pm 2.6$		$100.0 \pm 2.6$	$96.3 \pm 1.2$
$729.34 \pm 0.07$	E1	0.000005	$16.0 \pm 0.9$	$16.5 \pm 1.1$	$16.2 \pm 0.7$	$16.5 \pm 0.5$
$1375.8 \pm 0.06$	M1	0.000035	$36.9 \pm 1.5$	$37.5 \pm 1.5$	$37.2 \pm 1.1$	$36.4 \pm 0.6$
$1471.6 \pm 0.4$	E2	0.000080	$0.7 \pm 0.1$	$0.7 \pm 0.1$	$0.7 \pm 0.1$	$0.7 \pm 0.1$
$2473.96 \pm 0.03$	M1	0.00096	$19.9 \pm 1.5$	$22.8 \pm 1.1$	$21.8 \pm 0.9$	$20.7 \pm 0.7$
$2492.13 \pm 0.1$	M1	0.00045	$17.7 \pm 0.9$	$15.4 \pm 1.5$	$17.1 \pm 0.8$	$16.4 \pm 0.6$
$3137.58 \pm 0.21$	E1	0.00131	$19.2 \pm 1.1$	$18.0 \pm 1.1$	$18.6 \pm 0.8$	$16.5 \pm 0.5$
$3849.49 \pm 0.15$	E1	0.00162	$38.0 \pm 1.1$	$39.3 \pm 1.1$	$38.6 \pm 0.8$	$37.9 \pm 0.8$
$3867.6 \pm 0.3$	M1	0.00097	$5.7 \pm 0.8$	$5.2 \pm 1.1$	$5.5 \pm 0.6$	$5.4 \pm 0.6$
$3945.1 \pm 0.4$	E1	0.00166	$2.6 \pm 0.7$	$4.1 \pm 1.1$	$3.0 \pm 0.6$	$2.9 \pm 0.6$

<sup>a</sup>Constrained least-squares fit to the level scheme with a  $\chi^2/f = 1.25$ .

<sup>b</sup>Transition not observed. The transition probability is inferred from the decay scheme intensity balance.

TABLE VIII. Determination of the deuterium  $\gamma$  ray and total radiative thermal neutron capture cross sections.

	Calibration standard			$\sigma_\gamma(6250)$
	Isotope	$E_\gamma$	$\sigma_\gamma$ (mb)	(mb)
Target-1	$^{16}\text{O}$	870.76	$0.164 \pm 0.003$	$0.481 \pm 0.020$
Target-2	$^{16}\text{O}$	870.76	$0.164 \pm 0.003$	$0.483 \pm 0.020$
Urea	$^{14}\text{N}$	1884.85	$14.57 \pm 0.04$	$0.497 \pm 0.009$
Urea	$^{12}\text{C}$	4945.30	$2.62 \pm 0.03$	$0.478 \pm 0.012$
			Weighted average	$0.488 \pm 0.006^a$

<sup>a</sup>Correcting for the internal pair formation coefficient  $\alpha_{\text{IPF}} = 0.00164$  gives  $\sigma_0(\text{D}) = 0.489 \pm 0.006$ .

the four measurements of the  $^{18}\text{O}(n,\gamma)$  total radiative neutron cross section is  $\sigma_0(^{16}\text{O}) = 0.141 \pm 0.006$  mb

Three values from the literature,  $\sigma_0(^{18}\text{O}) = 0.22 \pm 0.04$  mb by Seren *et al.* [16],  $\sigma_0(^{18}\text{O}) = 0.16 \pm 0.01$  mb by Blaser *et al.* [17], and  $\sigma_0(^{18}\text{O}) = 0.16 \pm 0.01$  mb by Nagai *et al.* [18] are all considerably larger. The value from Nakai *et al.* [18] was standardized with respect to  $^{16}\text{O}$  assuming  $\sigma_0(^{16}\text{O}) = 0.187 \pm 0.010$  mb. Renormalizing their value to our new  $^{16}\text{O}$  cross section gives  $\sigma_0(^{18}\text{O}) = 0.14 \pm 0.01$  mb which agrees with the value determined here.

The neutron separation energy  $S_n = 3963.12 \pm 0.19$  keV determined in this experiment is significantly higher and more precise than the  $3955.6 \pm 2.6$  keV value reported in the most recent atomic mass evaluation [13].

#### 4. Deuterium cross section

The deuterated  $^{16,17,18}\text{O}$  targets were enriched to  $>99.9\%$  in deuterium (D). The  $\text{D}(n,\gamma)$  6250.24-keV  $\gamma$ -ray cross section can be determined from its intensity ratio to the 870.76-keV  $\gamma$  ray from  $^{16}\text{O}(n,\gamma)$ , whose cross section was discussed above, after correction for the  $^{16}\text{O}$  abundance in each target. We have also measured this cross section with a deuterated urea target

TABLE IX. Deuterium cross-section measurements.

Reference (year)	Method	Cross section (mb)
Sargent (1947) [21]	Pile oscillator	$0.92 \pm 0.22$
Kaplan (1952) [22]	Diffusion <sup>a</sup>	$0.572 \pm 0.10$
Jurney (1963) [10]	Capture $\gamma$ ray	$0.60 \pm 0.05$
Trail (1964) [23]	Capture $\gamma$ ray	$0.36 \pm 0.03$
Merritt (1967) [24]	Activation	$0.506 \pm 0.010$
Merritt (1968) [25]	Activation	$0.521 \pm 0.009$
Silk (1969) [26]	Diffusion	$0.523 \pm 0.029$
Ishikawa (1973) [27]	Activation	$0.55 \pm 0.10$
Alfimenkov (1980) [19]	NTOF	$0.487 \pm 0.024$
Jurney (1982) [20]	Capture $\gamma$ ray	$0.508 \pm 0.015$
Mughabghab (2006) [7]	Compilation	$0.508 \pm 0.015$
This work	Capture $\gamma$ ray	$0.489 \pm 0.006$

<sup>a</sup>Neglects the contribution of oxygen.

TABLE X. Total radiative neutron capture cross sections measured in this work.

Isotope	Cross section (mb)	
	Atlas [7]	This work
$^2\text{H}$	$0.508 \pm 0.015$	$0.489 \pm 0.006$
$^{16}\text{O}$	$0.190 \pm 0.019$	$0.170 \pm 0.003$
$^{17}\text{O}$	$0.538 \pm 0.065$	$0.67 \pm 0.07$
$^{18}\text{O}$	$0.16 \pm 0.01$	$0.141 \pm 0.006$

which can be standardized with respect to both nitrogen and carbon  $\gamma$  rays. The measurements of the  $\sigma_\gamma(6250)$  from these experiments are summarized in Table VIII.

The four measurements are consistent and give a weighted average value of  $\sigma_\gamma(6250) = 0.488 \pm 0.006$  mb including a statistical uncertainty of 1% and a calibration uncertainty of 0.7%. This cross section must be corrected for internal pair formation,  $\alpha_{\text{IPF}} = 0.00164$ , to obtain the total radiative neutron capture cross section  $\sigma_0(\text{D}) = 0.489 \pm 0.006$  mb. Previous measurements of the deuterium cross section are summarized in Table IX. Most earlier measurements are higher than the current value but the more recent values of Alfimenkov *et al.* [19] and Jurney [20], adopted by Mughabghab [7] are consistent with our new value.

### III. CONCLUSIONS

The total radiative neutron capture cross sections for  $^{16,17,18}\text{O}$  and deuterium have been measured by the PGAA method. Our new values are summarized in Table X where they are compared with the recommended values of Mughabghab [7]. Our new  $\sigma_0$  values for  $^{16,18}\text{O}$  and  $^2\text{H}$  were all significantly lower than most previous measurements. Unlike earlier measurements we have standardized our results using internal cross-section calibrations to get internally consistent, redundant results. These values were measured with two enriched targets and gave statistically consistent results confirming the reliability of the reported target isotopic abundances.

### ACKNOWLEDGMENTS

This work was performed under the auspices of the U.S. Department of Energy by the University of California, supported by the Director, Office of Science, Office of Basic Energy Sciences, of the U.S. Department of Energy at Lawrence Berkeley National Laboratory under Contract No. DE-AC02-05CH11231. We highly appreciate the enriched  $\text{D}_2^{17,18}\text{O}$  samples received from the Paul Scherrer Institut in Villigen, Switzerland.

- [1] Edited by G. Molnár, *Handbook of Prompt Gamma Activations Analysis with Neutron Beams* (Kluwer Academic Publishers, Boston, 2004).
- [2] P. Kudejova, G. Meierhofer, K. Zeitelhack, J. Jolie, R. Schulze, A. Turler, and T. Materna, *J. Radioanal. Nucl. Chem.* **278**, 691 (2008).
- [3] P. Kudejova, L. Canella, R. Schulze, N. Warr, A. Turler, and J. Jolie, *Proceedings of the Seventh International Conference on Nuclear and Radiochemistry, Budapest, Hungary 24–29 August, 2008* (Committee on Radiochemistry of the Hungarian Academy of Sciences (HAS), 2008).
- [4] T. Belgya, Z. Revay, I. H. B. Fazekas, L. Dabolczi, G. Molnár, J. O. Z. Kis, and G. Kaszás, in *Proceedings of the 9th International Symposium on Capture Gamma-Ray Spectroscopy and Related Topics, Budapest, Hungary, Oct. 8–12*, edited by G. Molnár, T. Belgya, and Zs. Révay (Springer-Verlag, Budapest/Berlin/Heidelberg, 1997), p. 826.
- [5] G. Molnár, Z. Revay, and T. Belgya, *Nucl. Instrum. Meth. Phys. Res. A* **489**, 140 (2002).
- [6] B. Fazekas, J. Óstór, Z. Kis, G. Molnár, and A. Simonits, in *Proceedings of the 9th International Symposium on Capture Gamma-Ray Spectroscopy and Related Topics, Budapest, Hungary, Oct. 8–12*, edited by G. Molnár, T. Belgya, and Zs. Révay (Springer-Verlag, Budapest/Berlin/Heidelberg, 1997), p. 774.
- [7] S. Mughabghab, *Atlas of Neutron Resonances*, 5th ed. (Elsevier, New York, 2006).
- [8] T. Kibedi, T. Burrows, M. Trzhaskovskaya, P. Davidson, and J. C.W. Nestor, *Nucl. Instr. and Meth. A* **589**, 202 (2008).
- [9] D. Tilley, H. Wellera, and C. Cheves, *Nucl. Phys. A* **564**, 1 (1993).
- [10] E. Journey and H. Motz, Argonne National Laboratory Report ANL-6797 (Argonne National Laboratory, Lemont, 1963), p. 236.
- [11] A. McDonald, E. Earle, M. Lone, F. Khanna, and H. Lee, *Nucl. Phys. A* **281**, 325 (1977).
- [12] N. Wüst, H. Seyfarth, and L. Aldea, *Phys. Rev. C* **19**, 1153 (1979).
- [13] M. Wang, G. Audi, A. Wapstra, F. Kondev, M. MacCormick, X. Xu, and B. Pfeiffer, *Chinese Phys. C* **36**, 1603 (2012).
- [14] M. Lone and W. Inglis, in *Proceedings of the International Symposium on Neutron Capture Gamma Ray Spectroscopy and Related Topics*, 3rd ed., edited by R. E. Chrien and W. R. Kane (Brookhaven National Laboratory, Upton, 1978), p. 678.
- [15] D. Tilley, H. Wellera, C. Cheves, and R. Chasteler, *Nucl. Phys. A* **595**, 1 (1995).
- [16] L. Seren, H. Friedlander, and S. Turkel, *Phys. Rev.* **72**, 888 (1947).
- [17] W. Blaser, A. Wytttenbach, and P. Baertschi, *J. Inorg. Nucl. Chem.* **33**, 1221 (1971).
- [18] Y. Nagai, M. Segawa, T. Ohsaki, H. Matsue, and K. Muto, *Phys. Rev. C* **76**, 051301 (2007).
- [19] V. Alfimenkov, S. Borzakov, J. Wierzbicki, B. Osipenko, L. Pikelner, V. Tishin, and E. Sharapov, NBS Special Publications **594**, 394 (1980).
- [20] E. T. Journey, P. J. Bendt, and J. C. Browne, *Phys. Rev. C* **25**, 2810 (1982).
- [21] B. Sargent, D. Booker, P. Cavanagh, H. Hereward, and N. Niemi, *Can. J. Res. A* **25**, 134 (1947).
- [22] L. Kaplan, G. Ringo, and K. Wilzbach, *Phys. Rev.* **87**, 785 (1952).
- [23] C. Trail and S. Raboy, Argonne National Laboratory Report ANL-6797 (Argonne National Laboratory, Lemont, 1963), p. 247.
- [24] J. Merritt, J. Taylor, and A. Boyd, *Nucl. Sci. Eng.* **28**, 286 (1967).
- [25] J. Merritt, J. Taylor, and A. Boyd, *Nucl. Sci. Eng.* **34**, 195 (1968).
- [26] M. Silk and B. Wade, *J. Nucl. Ener.* **23**, 625 (1969).
- [27] H. Ishikawa, *Nucl. Instrum. Meth.* **109**, 493 (1973).